Progress In Electromagnetics Research B, Vol. 18, 381–399, 2009

ASED-AIM ANALYSIS OF SCATTERING BY LARGE-SCALE FINITE PERIODIC ARRAYS

L. Hu, L.-W. Li, and T.-S. Yeo

Department of Electrical and Computer Engineering
National University of Singapore
Singapore 119260, Singapore

Abstract—In this paper, the Adaptive Integral Method (AIM) has been extended to characterizing electromagnetic scattering by large scale finite periodic arrays with each cell comprising of either dielectric or metallic objects, by utilizing accurate sub-entire-domain (ASED) basis function. The solution process can be carried out in two steps. In the first step, a small problem is solved in order to construct ASED basis functions to be implemented for the second step. When dielectric materials are involved in the cell which results in a large number of unknowns for the small problem, the AIM can be used to accelerate the solution process and reduce the memory requirement. In the second step, the entire problem is solved using the ASED basis function constructed in the first step. The AIM can be enhanced with the ASED basis function implemented to solve the entire problem more efficiently. When calculating the near interaction impedance matrix, computation time can be significantly reduced by using the near impedance matrix in the first step. The complexity analysis shows that the computational time is $O(N_0 \log N_0) + O(M \log M)$ and memory requirement is $O(N_0) + O(M)$, where N_0 denotes the number of cells and M stands for the number of elements in one cell. The results calculated respectively by the ASED-AIM and the existing AIM are then compared and an excellent agreement has been observed, which demonstrates the accuracy of the proposed method. In the meantime, memory and computational time requirements have been considerably reduced using the ASED-AIM as compared to the existing AIM. Finally, an example with over 10 million unknowns is given to demonstrate the efficiency of the proposed method.

Corresponding author: L. Hu (huli@nus.edu.sg).

1. INTRODUCTION

There has been always a desire of developing fast solvers to alleviate the stringent computational and memory requirements for various engineering and scientific applications. When using the method of moments (MoM) to solve electromagnetic scattering problems, the resultant integral equations will usually lead to a dense matrix in the large-dimensional linear system and they are usually solved by iterative solvers such as Conjugate Gradient Method. The direct solver requires $O(N^3)$ operations to solve such linear equations with the number N of unknowns, while the iterative solver requires $O(N_{\text{iter}}N^2)$ operations where N_{iter} denotes the number of iterations. Both methods require $O(N^2)$ memory to store the dense matrices. Thus, the stringent computational and memory requirements have impeded the MoM from solving large-scale problems which prevails in real life. Until now, there are two kinds of fast solvers which are commonly adopted in the electromagnetics community.

The first type of approaches includes Fast Multipole Method (FMM) [1–3] and its extension, Multilevel Fast Multipole Algorithm (MLFMA) [4–6] which were developed based on the addition theorem and spherical multipole expansion. The second type of methods was developed based on fast Fourier transforms and it includes the Conjugate Gradient FFT (CG-FFT) method, the Adaptive Integral Method (AIM), and the pre-corrected fast Fourier transform (pFFT) method.

The CG-FFT method was developed and extended by [7–11]. The attracting feature of this method is that the computational and memory requirements are $O(N \log N)$ and $O(N)$, respectively. But its major drawback is the staircase approximation, that is, the uniform meshed grids assumed to represent the arbitrarily shaped objects. This assumption results in the staircase error and affects considerably the accuracy of the approach. In order to overcome the staircase approximation of CG-FFT method, the Adaptive Integral Method (AIM) was developed by [12]. The AIM has been successfully applied in scattering problems associated with general objects such as perfectly electric conducting (PEC) objects [13], dielectric objects [14], composite dielectric and PEC objects [15], magnetodielectric objects [16] and so on. The precorrected-FFT (pFFT) method was proposed to solve the Laplace equation for static problem of analyzing very large scale integrated circuits [17, 18]. The pFFT method has then extended to solve the vectorial Helmholtz equations for electromagnetic scattering problems [19] and it has been applied successively to the solution of the SIE formulation

for large conducting objects [20–22], and mixed conducting-dielectric objects [23, 24]. Recently it was extended to the analysis of inhomogeneous dielectric objects by using the VIE formulation [25, 26], the hybrid volume surface integral equation for the analysis of composite conducting and dielectric objects, and various antenna analysis [27–30]. Although the pFFT method is very similar to the AIM, they were originated differently in different areas, but almost at the same time; most importantly, they have different mapping schemes, which thus differentiates the two approaches.

Large-scale finite periodic structures have been topics of considerable interests and various novel industrial, academic and scientific applications. Therefore, accurate and fast analysis of these structures are very important. However, full wave simulations for these structures, even with the aid of the available fast solvers, are very difficult since important properties (such as periodicity) are not used in conventional solvers. Recently, some novel physics-based basis function have been proposed to solve these challenging problems such as sub-domain multilevel approach [31], synthetic basis function [32], characteristic basis function [33–35] and accurate sub-entire-domain (ASED) basis function [36–38]. In the present work, We adopt the ASED basis function because it is specially tailored to periodic structures and it considers the most important coupling among the nearest neighboring cells which is neglected by simplified sub-entire-domain (SSED) basis function and thus is more accurate than the latter [36]. Two stages are required using ASED basis function to solve the scattering problems by finite periodic arrays. The first step work is to consider the most important mutual coupling among the nearest neighbors to obtain the ASED basis function and the second step work is to quantify the overall interactions of all elements based on the ASED basis function. The ASED method has been accelerated using CG-FFT [37] and it was later combined with the FMM to significantly reduce memory requirement and computational complexity of FMM in solving periodic array problems [38].

In this paper, we propose a new AIM approach to solve the electromagnetic scattering by large-scale periodic arrays whose elements are made of composite metallic and dielectric materials. Therefore, this method can be used to characterize frequency selective surfaces, photonic crystals and metamaterials with a large but finite number repeating or periodic elements. The new approach, which is referred to as the ASED-AIM, has all advantages of both ASED basis functions and AIM. Since the ASED basis function is associated with each cell of the periodic structures, number of unknowns have been considerably reduced from MN_0 to N_0 where M denotes the number

of unknowns in each cell while N_0 stands for the number of cells in the periodic structures. In the subsequent sections, we first formulate the problem using the ASED-AIM algorithm for solving large-scale finite periodic arrays comprising of metallic and dielectric objects. The algorithm takes two steps in development. The first step is to obtain the ASED basis function and the second step is to solve the entire problem using the ASED basis function. In [38], disaggregation, aggregation and translation have to be performed in k directions, which needs $O(M)$ times per iteration. In the presently proposed ASED-AIM method, interpolation, projection and FFT only need to be carried out once or twice per iteration. Thus, computational time can be considerably reduced. Therefore, the computational time saving scheme will be illustrated for calculating the near-field interaction impedance matrix in the second step. Complexity analysis reveals that in the present analysis, the memory requirement is $O(M)+O(N_0)$ while the computational time is $O(M \log M) + O(N_0 \log N_0)$. Numerical results demonstrate the accuracy and efficiency ASED-AIM in solving finite array problems where one example with over 10 million unknowns has been shown.

2. ASED-AIM FORMULATION

Electromagnetic scattering, by and propagation in, periodic conducting objects such as frequency selective surfaces, periodic dielectric objects such as photonic crystals, and periodic composite or hybrid conducting and dielectric objects such as metamaterials can be characterized using volume-surface integral equation (VSIE) method. The basic equations are formulated below via the boundary conditions satisfied by electric and magnetic field tangential components:

$$\mathbf{E}^i(\mathbf{r}) = \mathbf{E}(\mathbf{r}) - \mathbf{E}^s(\mathbf{r}), \quad \mathbf{r} \in V \tag{1}$$

$$\mathbf{E}^i(\mathbf{r})\big|_{\tan} = -\mathbf{E}^s(\mathbf{r})|_{\tan}, \quad \mathbf{r} \in S. \tag{2}$$

Equivalent electric volume current $\mathbf{J}_V(\mathbf{r})$ and equivalent electric surface current $\mathbf{J}_S(\mathbf{r})$ are related to total electric field $\mathbf{E}(\mathbf{r})$ and scattered electric field $\mathbf{E}^s(\mathbf{r})$ via

$$\mathbf{J}_V(\mathbf{r}) = j\omega\kappa\mathbf{D}(r) = j\omega(\epsilon - \epsilon_0)\mathbf{E}(r), \quad \mathbf{r} \in V \tag{3}$$

$$\mathbf{E}^s(\mathbf{r}) = -j\omega\mu_0 \int_V G(\mathbf{r},\mathbf{r}')\mathbf{J}_V(\mathbf{r}')dV' - j\omega\mu_0 \int_S G(\mathbf{r},\mathbf{r}')\mathbf{J}_S(\mathbf{r}')dS'$$
$$+\frac{\nabla}{j\omega\epsilon_0} \int_V G(\mathbf{r},\mathbf{r}')\nabla' \cdot \mathbf{J}_V(\mathbf{r}')dV' + \frac{\nabla}{j\omega\epsilon_0} \int_S G(\mathbf{r},\mathbf{r}')\nabla' \cdot \mathbf{J}_S(\mathbf{r}')dS' \tag{4}$$

where $G(\mathbf{r},\mathbf{r}')$ denotes free space Green's function, μ_0 and ϵ_0 represent free space permeability and permittivity respectively, ϵ stands for

permittivity in the dielectric object, and $\kappa = (\epsilon - \epsilon_0)/\epsilon$ identifies the contrast ratio of scatterer material and its background medium.

For simplicity, we consider 2D large scale periodic structures. Three dimensional periodic problems can be analyzed in the same fashion. Based on the ASED method, we can first solve an electrically small problem with nine cells for 2D periodic structures. Then, we will use the solution to construct the basis function for each cell and then solve the entire problem of large scale. If there are M unknowns for each cell and $N_0 = N_x N_y$ cells, the total number of unknowns will be MN_0. This number of unknowns can be significantly reduced to N_0 via the ASED method. For the p-th cell, surface currents can be expanded, in order to ensure the normal continuity of surface current in the metallic surface, as follows:

$$\mathbf{J}_p^S = \sum_{m=1}^{N_S} I_{p_m}^S \mathbf{f}_{p_m}^S; \tag{5}$$

in order to ensure the normal continuity of electric flux density inside the dielectric objects, $\mathbf{D}_p$ can be expanded as:

$$\mathbf{D}_p = \frac{1}{j\omega} \sum_{m=1}^{N_V} I_{p_m}^V \mathbf{f}_{p_m}^V; \tag{6}$$

thus, volume currents can be expanded as

$$\mathbf{J}_p^V = \sum_{m=1}^{N_V} I_{p_m}^V \kappa \mathbf{f}_{p_m}^V; \tag{7}$$

where $\mathbf{f}_{p_m}^S$ and $\mathbf{f}_{p_m}^V$ denote respectively the RWG and SWG basis functions associated with the m-th surface and volume basis functions of the p-th cell, N_S is the number of RWG basis functions while N_V is the number of SWG basis functions, and $I_{p_m}^S$ and $I_{p_m}^V$ stand for the respective unknown coefficients to be solved for. Thus, electric current for the p-th cell can be written as

$$\mathbf{J}_p = \mathbf{J}_p^S + \mathbf{J}_p^V. \tag{8}$$

The total current for the nine cell problem can be written as

$$\mathbf{J} = \sum_{p=1}^{9} \mathbf{J}_p. \tag{9}$$

We use the Galerkin procedure of MoM to test the volume-surface integral equations and obtain the following matrix equations:

$$[Z_{p_m q_n}]\,[I_{q_n}] = [V_{p_m}] \tag{10}$$

where p_m denotes the m-th testing function in the p-th cell while q_n stands for the n-th basis function in the q-th cell. The impedance matrix $\bar{Z}$ comprises of 9×9 sub-matrices of size $M \times M$ with the p-th block row and the q-th block column representing the interaction among elements inside the (p, q)-th cell, where M denotes the total unknown number in a cell. For the p-th block row and q-th block column sub-matrix, it can be written in terms of following block matrices

$$[Z_{p_m q_n}] = \begin{bmatrix} Z^{VV}_{p_m q_n} & Z^{VS}_{p_m q_n} \\ Z^{SV}_{p_m q_n} & Z^{SS}_{p_m q_n} \end{bmatrix} \tag{11}$$

whose detailed block matrix expressions can be written as

$$Z^{VV}_{p_m q_n} = \frac{1}{j\omega} < \mathbf{f}^V_{p_m},\ \frac{1}{\epsilon}\mathbf{f}^V_{q_n} > + j\omega\mu_0 < \mathbf{f}^V_{p_m},\ \mathbf{A}^V_{q_n} > \tag{12}$$

$$-\frac{1}{j\omega\epsilon_0} < \mathbf{f}^V_{p_m},\ \nabla\phi^V_{q_n} > \tag{13}$$

$$Z^{VS}_{p_m q_n} = j\omega\mu_0 < \mathbf{f}^V_{p_m},\ \mathbf{A}^S_{q_n} > -\frac{1}{j\omega\epsilon_0} < \mathbf{f}^V_{p_m},\ \nabla\phi^S_{q_n} > \tag{14}$$

$$Z^{SV}_{p_m q_n} = j\omega\mu_0 < \mathbf{f}^S_{p_m},\ \mathbf{A}^V_{q_n} > -\frac{1}{j\omega\epsilon_0} < \mathbf{f}^S_{p_m},\ \nabla\phi^V_{q_n} > \tag{15}$$

$$Z^{SS}_{p_m q_n} = < \mathbf{f}^S_{p_m},\ \mathbf{f}^S_{q_n} > + j\omega\mu_0 < \mathbf{f}^S_{p_m},\ \mathbf{A}^S_{q_n} >$$

$$-\frac{1}{j\omega\epsilon_0} < \mathbf{f}^S_{p_m},\ \nabla\phi^S_{q_n} > \tag{16}$$

where

$$\mathbf{A}^V_{q_n} = \int_V G\mathbf{f}^V_{q_n} dV' \tag{17}$$

$$\mathbf{A}^S_{q_n} = \int_S G\mathbf{f}^S_{q_n} dS' \tag{18}$$

$$\phi^V_{q_n} = \int_V G\nabla' \cdot \mathbf{f}^V_{q_n} dV' \tag{19}$$

$$\phi^S_{q_n} = \int_S G\nabla' \cdot \mathbf{f}^S_{q_n} dS'. \tag{20}$$

This equation can be solved using the AIM when M becomes large. After solving the nine-cell problem, we can obtain the nine types of cell basis functions and the use them to solve the entire problem. Now the current density can be written as

$$\mathbf{J} = \sum_{p=1}^{N_0} j_p \mathbf{J}_p \tag{21}$$

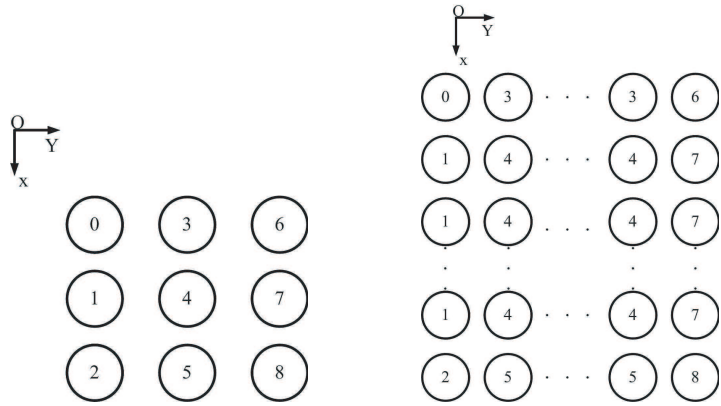

Figure 1. Mapping of the ASED basis functions. (a) The nine-cell problem; (b) The entire problem.

where j_p denotes unknowns to be solved for. The cell impedance matrix elements (denoted by the superscript C herein and subsequently) can be written as

$$Z_{pq}^{C} = \sum_{m=1}^{M} \sum_{n=1}^{M} I_{p_m} Z_{p_m q_n} I_{q_n}. \tag{22}$$

Although there are N_0 cells in the whole domain, only nine types of basis functions will be utilized. These nine types of basis functions can be mapped onto the entire domain shown in Fig. 1.

When N_0 is large, we can use the AIM to accelerate the solution process. We should combine the ASED approach with the AIM to solve large-scale periodic structure problems. The basic idea of AIM is to calculate the far-zone interaction via projecting the basis functions to, and interpolating potentials from, grid space associated with each basis function while the near zone interactions can be directly calculated. Since free space Green's function is translational invariant and the calculation is made based on grid space, the FFT can be used to greatly reduce the memory requirement and computational time. Using the conventional AIM, the matrix vector multiplication can be written as

$$\bar{Z}\mathbf{I} = \bar{\mathbf{V}}\ \bar{\mathbf{H}}\ \bar{\mathbf{P}}\ \mathbf{I} + \bar{Z}^{\text{near}}\mathbf{I} \tag{23}$$

where $\bar{\mathbf{V}}$ is the interpolation matrix, $\bar{\mathbf{H}}$ is the Green's function matrix, and $\bar{\mathbf{P}}$ is the projection matrix. The mapping and calculations are made using the following four steps:

(i) to project the sources distributed on the basis functions onto the regular grids by matching their vector and scalar potentials at

some given test points to guarantee the approximate equality of their far fields;

(ii) to evaluate the potentials at other grid locations produced by these grid-projected sources by a 3-D convolution;

(iii) to interpolate the grid point potentials onto the testing functions, where the projection and interpolation operators are represented by sparse matrices, and the convolution can be carried out rapidly using discrete FFTs; and

(iv) to compute the near-field interactions directly and remove the errors introduced by the far-field operators.

The four steps of conventional AIM can be shown in Fig. 2.

For the far zone interaction, the impedance matrix elements can be approximated as:

$$Z_{p_m q_n} \approx \tilde{Z}_{p_m q_n} = \sum_s \sum_t V_{m_s} H_{m_s n_t} P_{n_t} \tag{24}$$

where $\sum$ denotes summation of all the grids associated with the basis functions. Thus, for cell interaction in the far zone, we have

$$\begin{aligned} Z_{pq}^C &= \sum_m \sum_n I_{p_m} Z_{p_m q_n} I_{q_n} \\ &\approx \sum_m \sum_s \sum_n \sum_t I_{p_m} V_{m_s} H_{m_s n_t} I_{q_n} P_{n_t} \\ &= V_p^C H_{pq} P_q^C \end{aligned} \tag{25}$$

where $\bar{\mathbf{V}}^C$ and $\bar{\mathbf{P}}^C$ are the interpolation and projection matrices for cell basis functions. They can be written explicitly as:

$$V_p^C = \sum_m \sum_s I_{p_m} V_{m_s} \tag{26}$$

$$P_q^C = \sum_n \sum_t I_{q_n} P_{n_t}. \tag{27}$$

Now, Using the ASED-AIM, the matrix vector multiplication can be written as

$$\bar{\mathbf{Z}}^C \cdot \bar{\mathbf{I}}^{\mathbf{C}} = \bar{\mathbf{V}}^{\mathbf{C}} \cdot \bar{\mathbf{H}} \cdot \bar{\mathbf{P}}^{\mathbf{C}} \cdot \bar{\mathbf{I}}^{\mathbf{C}} + \bar{\mathbf{Z}}^{C,\text{near}} \cdot \bar{\mathbf{I}}^C \tag{28}$$

which takes the four steps to manipulate as follows:

(i) to sum-up all the projections from every basis functions within each cell;

(ii) to evaluate the potentials at other grid locations produced by these grid-projected sources using a 3-D convolution;

(iii) to interpolate the grid point potentials onto each cell rather than individual testing functions; and

(iv) to compute the near-field interactions directly from at most nine near-by neighbors.

The four steps for implementing the ASED-AIM is shown graphically in Fig. 3.

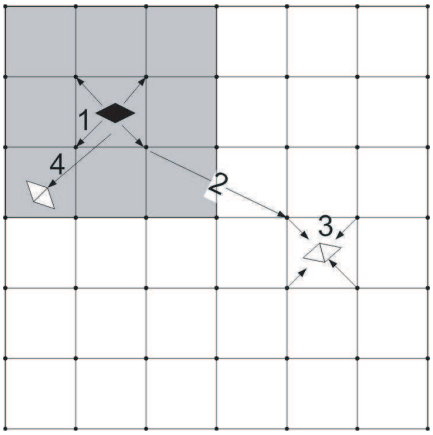

Figure 2. The pictorial representation of the conventional AIM. Step 1 denotes the projection of basis functions to associated grids; Step 2 stands for the grid potential calculation using the FFT; Step 3 represents the interpolation of grid potentials to testing functions; and Step 4 identifies the direct calculation of near zone interactions. Shaded area denotes the near zone for the basis function in black at the upper left corner.

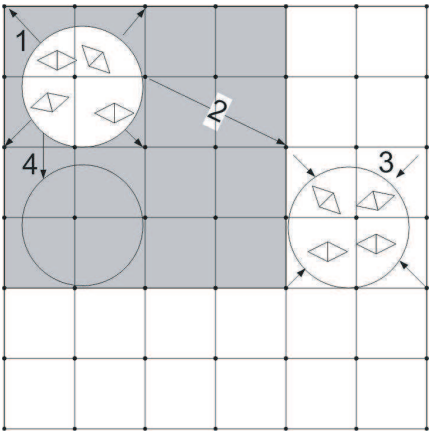

Figure 3. The pictorial representation of the ASED-AIM. Step 1 denotes the sum of projection of basis functions in each cell; Step 2 stands for the grid potential calculation using the FFT; Step 3 represents the interpolation of grid potential to each cell rather than each testing function; and Step 4 identifies the direct calculation of near zone interactions, each cell has at most nine nearest neighbors. Shaded area denotes the near interaction for the white cell at the upper left corner.

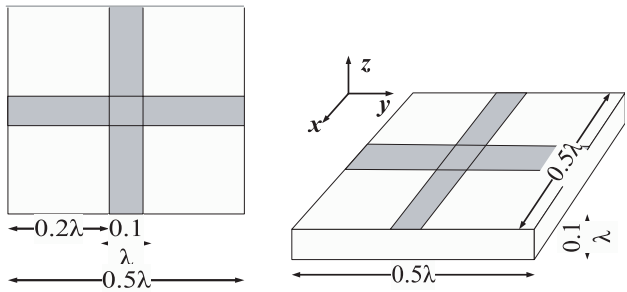

Figure 4. The unit cell of arrays in this paper. (a) Top view; (b) 3D view. The cell is made up of a dielectric cuboid with width 0.5λ, length 0.5λ and height 0.1λ. The permittivity for the cuboid is $\epsilon_r = 2$. On top of the cuboid there is a metallic cross with parameters shown in the figure.

3. COMPUTATIONAL COMPLEXITY AND MEMORY REQUIREMENT FOR ASED-AIM

In the first step of ASED-AIM, the conventional AIM is carried out to solve a problem with $9M$ unknowns. Thus, the memory requirement and computational time are $O(M)$ and $O(M\log(M))$, respectively. When composite metallic and dielectric objects are within a cell since M is large, for example, $M = 10^3$, this portion of memory and computational time should be taken into consideration as can be shown in the numerical results later. In the second step of ASED-AIM, since there are only nine types of cell basis functions, the memory requirement for interpolation and projection matrix is a constant C and the computational time is $O(N_0)$ where N_0 denotes the number of cells in the whole domain. For the FFT operation, since the grid number Ng is proportional to the total number of cells N_0, thus the memory requirement is $O(N_0)$ and the computational time is $O(N_0 \log N_0)$.

In [38], disaggregation (equivalent to interpolation in the AIM), aggregation (equivalent to projection in the AIM) and translation (equivalent to the FFT in the AIM) have to be carried for each k direction (which is of order M) respectively per iteration. However, interpolation, projection only need once and the FFT twice per iteration in the AIM. Thus, the computational time can be reduced greatly. For the near interaction, the computational time will be quite large if we calculate directly using

$$Z_{pq}^{C,\text{near}} = Z_{pq}^{C} - \widetilde{Z}_{pq}^{C} = \sum_{m=1}^{M}\sum_{n=1}^{M} I_{p_m}\left(Z_{p_m q_n} - \tilde{Z}_{p_m q_n}\right) I_{q_n} \tag{29}$$

since this operation takes $O(M^2)$ multiplication and addition. In fact, we can utilize the near zone interaction matrix Z^{near} in the first step. We know that Z^{near} is a sparse $9M \times 9M$ matrix, which is made up of 9×9 sub-matrices with each matrix $M \times M$ elements, each element is $(Z_{p_m q_n} - \tilde{Z}_{p_m q_n})$. Consider the fifth row of the sub-matrices which are calculated when the cell p is surrounded by nine most near neighboring cells q, as shown in Fig. 1(a) where $p = 4$ and $q = 0, \ldots, 8$. The sub-matrices are all sparse, since

$$Z_{p_m q_n} - \tilde{Z}_{p_m q_n} = 0, \quad d_{p_m q_n} > d_{\text{near}} \tag{30}$$

where d_{near} is the near zone threshold. Thus, $O(M^2)$ multiplications and additions can be greatly reduced using sparse matrix vector multiplication. For the near zone interactions, there are at most nine near neighbors for each cell; thus the memory requirement and the computational time are $O(N_0)$. Thus, the total memory requirement is

$$O(M) + C + O(N_0) + O(N_0) = O(M) + O(N_0); \tag{31}$$

and the total computational time is

$$\begin{aligned} & O(M \log M) + O(N_0) + O[N_0 \log(N_0)] + O(N_0) \\ = \; & O(M \log M) + O[N_0 \log(N_0)]. \end{aligned} \tag{32}$$

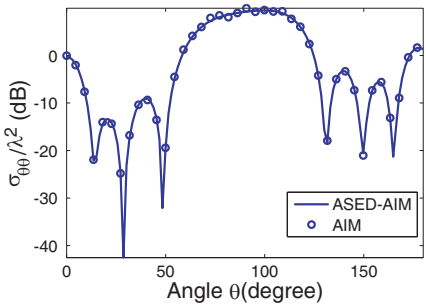

Figure 5. Bistatic RCS values of the 4×4 array with each cell shown in Fig. 4, incident by θ-polarized plane wave with the grazing incident angle $\theta_i = 90°$ and $\phi_i = 0°$. The gap is 0.5λ in both x- and y-directions. The results are computed using the AIM (circle line) and the ASED-AIM (solid line).

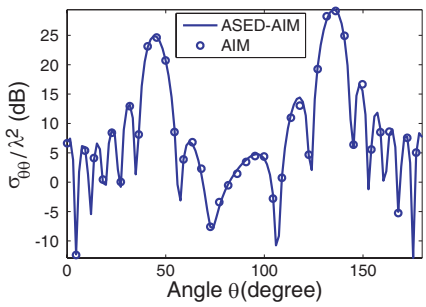

Figure 6. Bistatic RCS values of the 8×8 array with each cell shown in Fig. 4, incident by θ-polarized plane wave with the oblique incident angle $\theta_i = 45°$ and $\phi_i = 0°$. The gap is 0.5λ in both x- and y-directions. The results are computed using the AIM (circle line) and the ASED-AIM (solid line).

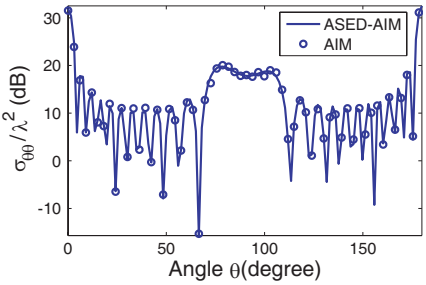

Figure 7. Bistatic RCS values of the 12×12 array with each cell shown in Fig. 4, incident by θ-polarized plane wave with the normal incident angle $\theta_i = 0^\circ$ and $\phi_i = 0^\circ$. The gap is 0.2λ in both x- and y-directions. The results are computed using the AIM (circle line) and the ASED-AIM (solid line).

4. NUMERICAL RESULTS

In this section, several examples will be given to demonstrate the validity and efficiency of our code to solve electromagnetic scattering by large scale periodic structures consisting of composite metallic and dielectric objects. The GMRES solver is adopted as the iterative solver and it terminates when the normalized residue falls below 10^{-3}.

In the first case, we consider a 4×4 array incident by θ-polarized plane wave with the grazing incident angle $\theta_i = 90^\circ$ and $\phi_i = 0^\circ$. Comparison is made between the ASED-AIM result and the AIM result and an excellent agreement has been observed. The number of unknowns for the 4×4 array is 17,296 and it requires memory of 125 MB and computational time of 34 seconds when the ASED-AIM is used, while it needs memory of 222 MB and computational time of 112 seconds when the conventional AIM is utilized.

In the second example, we consider a 8×8 array incident by θ-polarized plane wave with the oblique incident angle $\theta_i = 45^\circ$ and $\phi_i = 0^\circ$. Comparison is made between the ASED-AIM result and the AIM result and an excellent agreement has been observed. The number of unknowns for the 8×8 array is 69,184 and it requires memory of 128 MB and computational time of 38 seconds when the ASED-AIM is used, while it needs memory of 888 MB and computational time of 479 seconds when the conventional AIM is utilized.

As a third example, we consider a 12×12 array incident by θ-polarized plane wave with the normal incident angle $\theta_i = 0^\circ$ and $\phi_i = 0^\circ$. Comparison is made between the ASED-AIM result and the AIM result and an excellent agreement has been observed. The number

of unknowns for the 12×12 array is 155,664 and it requires memory of 132 MB and computational time of 42 seconds when the ASED-AIM is used, while it needs memory of 2,000 MB and computational time of 1,167 seconds when the conventional AIM is utilized.

From these cases, it is clear that when solving scattering by arrays with different sizes and under arbitrarily incident plane waves, ASED-AIM results agree well with conventional AIM results. However, the memory requirement and CPU time are almost the same when the ASED-AIM is applied, while the memory requirement and CPU time increase proportionally to the array sizes when the conventional AIM is utilized.

Subsequently, we investigate the computational complexity and memory requirement of the ASED-AIM and the compare them with those of the conventional AIM. Fig. 8 shows the relationship between the computational time and the number of unknowns using the ASED-AIM and the AIM. Fig. 9 shows the relationship between the memory and the number of unknowns using the ASED-AIM and the AIM. From these in Figs. 8 and 9, it is clear that when the AIM is used, the computational time and the memory requirement are proportional to the number N of unknowns. When N reaches 10^5, the memory requirement is over 10^3 MB and CPU time is over 10^3 seconds. When the ASED-AIM is used, the computational time and the memory requirement are much less than those when the conventional AIM is used, even when N reaches 10 million, the memory requirement is still less than 10^3 MB and CPU time is less than 10^3 seconds. Especially, they are nearly the same when the number of unknowns

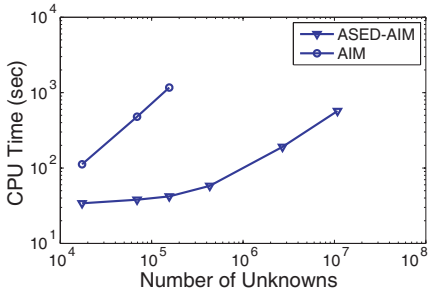

Figure 8. The relationship between computational time and the number of unknowns within the ASED-AIM (triangle line) and the AIM (circle line).

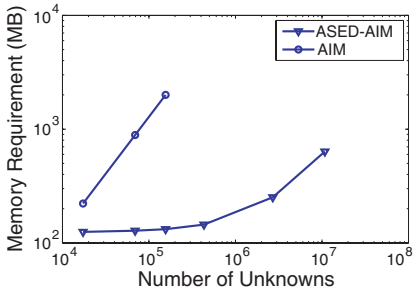

Figure 9. The relationship between memory requirement and the number of unknowns within the ASED-AIM (triangle line) and the AIM (circle line).

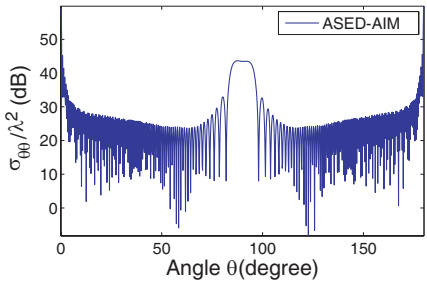

Figure 10. Bistatic RCS values of the 100×100 array with each cell shown in Fig. 4, incident by θ-polarized plane wave with the normal incident angle $\theta_i = 0^\circ$ and $\phi_i = 0^\circ$. The gap is 0.5λ in both x- and y-directions.

is less than 10^6. When the number of unknowns goes up beyond 10^6, the memory requirement and the CPU time become proportional to the number of unknowns. This observation agrees well with the previous complexity analysis in literature. Since the memory requirement is $O(M)+O(N_0)$, the computational time is $O(M \log M)+O(N_0 \log N_0)$, where M denotes the number of unknowns in each cell while N_0 stands for the number of cells in the periodic structures. When N_0 is small as compared to M, M determines the memory requirement and computational time. It means that most of CPU time and memory have been spent on the first stage of the ASED-AIM. From our results, 120 MB memory and 30 seconds computational time have been used in the first stage. When N is smaller than 10^6, only several MB of memory and a few seconds of computational time have been used in the seconds stage. When N is larger than 10^6, effect of N_0 becomes dominant. The memory requirement and CPU time both increase linearly with N.

Finally, we consider we consider a 100×100 array incident by θ-polarized plane wave with the normal incident angle $\theta_i = 0^\circ$ and $\phi_i = 0^\circ$. The total number of unknowns in this example is 10.81 million. The calculated radar cross section is shown in Fig. 10. For such an electrically large structure with over 10 million unknowns, the ASED-AIM only requires 636 MB memory and 570 seconds, which demonstrates the efficiency of the new method in solving problems of electromagnetic scattering by large-scale periodic structures.

5. CONCLUSION

In this paper, an extended AIM algorithm has been developed based on the ASED basis functions to solve problems of electromagnetic

scattering by large-scale finite periodic arrays comprising of metallic and dielectric objects. The volume-surface integral equation is used to characterize the scattering property of periodic arrays. Two steps are needed in the ASED-AIM to solve the large array problems. The first step is to solve a small-scale problem with nine cells. We obtain the ASED basis function after the first step is completed. In the second step, we use the ASED basis function for each cell and then solve the entire problem. The AIM has been thus modified to incorporate the ASED basis function which reduces the memory requirement and computational time significantly in solving the array problems. Complexity analysis reveals that in the new algorithm, the memory requirement is $O(M) + O(N_0)$ and the computational time is $O(M \log M) + O(N_0 \log N_0)$ where M is the number of unknowns in each cell and N_0 is the number of cells in the whole array. Numerical results further demonstrate the accuracy and efficiency of the ASED-AIM in comparison with conventional AIM in solving finite array problems. One example with over 10 million unknowns is successfully considered and its numerical results are illustrated.

ACKNOWLEDGMENT

The authors are grateful to the Defence Science and Technology Agency of Singapore and the National University of Singapore for the financial support in terms of Defence Innovative Research Program with Project No: DSTA-NUS-DIRP/2007/02.

REFERENCES

1. Rokhlin, V., "Rapid solution of integral equations of scattering theory in two dimensions," *J. Comput. Phys.*, Vol. 86, No. 2, 414–439, Feb. 1990.
2. Coifman, R., V. Rokhlin, and S. Wandzuraz, "The fast multipole method for the wave equation: A pedestrian prescription," *IEEE Trans. Antennas Propagat.*, Vol. 35, No. 3, 7–12, Jun. 1993.
3. Engheta, N., W. D. Murphy, V. Rokhlin, and M. S. Vassiliou, "The fast multipole method (FMM) for electromagnetic scattering problems," *IEEE Trans. Antennas Propagat.*, Vol. 40, 634–641, Jun. 1992.
4. Lu, C. C. and W. C. Chew, "A fast algorithm for solving hybrid integral equation," *IEE Proceedings-H*, Vol. 140, No. 6, 455–460, Dec. 1993.
5. Song, J., C.-C. Lu, and W. C. Chew, "Multilevel fast multipole

algorithm for electromagnetic scattering by large complex objects," *IEEE Trans. Antennas Propagat.*, Vol. 45, No. 10, 1488 –1493, Oct 1997.

6. Cui, T. J., W. C. Chew, G. Chen, and J. M. Song, "Efficient MLFMA, RPFMA and FAFFA algorithms for EM scattering by very large structures," *IEEE Trans. Antennas Propagat.*, Vol. 52, No. 3, Mar. 2004.
7. Sarkar, T. K., E. Arvas, and S. M. Rao, "Application of FFT and the conjugate gradient method for the solution of electromagnetic radiation from electrically large and small conducting bodies," *IEEE Trans. Antennas Propagat.*, Vol. 34, No. 5, 635–640, May 1986.
8. Peters, T. J. and J. L. Volakis, "Application of a conjugate gradient FFT method to scattering from thin planar material plates," *IEEE Trans. Antennas Propagat.*, Vol. 36, No. 4, 518–526, Apr. 2000.
9. Catedra, M. F., J. G. Cuevas, and L. Nuno, "A scheme to analyze conducting plates of resonant size using the conjugate gradient method and the fast Fourier transform," *IEEE Trans. Antennas Propagat.*, Vol. 36, No. 12, 1744–1752, Dec. 1988.
10. Zwamborn, P. and P. V. Den Berg, "Three dimensional weak form of the conjugate gradient FFT method for solving scattering problems," *IEEE Trans. Microwave Theory Tech.*, Vol. 40, No. 9, 1757–1766, 1992.
11. Cui, T. J. and W. C. Chew, "Fast algorithm for electromagnetic scattering by buried 3-D dielectric objects of large size," *IEEE Trans. Geosci. Remote Sensing*, Vol. 37, 2597–2608, Sep. 1999.
12. Bleszynski, E., M. Bleszynski, and T. Jaroszewicz, "AIM: Adaptive integral method for solving large-scale electromagnetic scattering and radiation problems," *Radio Sci.*, Vol. 31, No. 5, 1225–1252, 1996.
13. Wang, C. F., F. Ling, J. Song, and J. M. Jin, "Adaptive integral solution of combined field integral equation," *Microwave Opt. Technol. Lett.*, Vol. 19, No. 5, 321–328, Dec. 1998.
14. Zhang, Z. Q. and Q. H. Liu, "A volume adaptive integral method (VAIM) for 3-D inhomogeneous objects," *IEEE Antennas and Wireless Propagat. Lett.*, Vol. 1, No. 5, 102–105, 2002.
15. Ewe, W.-B., L.-W. Li, and M.-S. Leong, "Fast solution of mixed dielectric/conducting scattering problem using volume-surface adaptive integral method," *IEEE Trans. Antennas Propagat.*, Vol. 52, No. 11, 3071–3077, Nov. 2004.

16. Ewe, W.-B., E.-P. Li, H.-S. Chu, and L.-W. Li, "AIM analysis of electromagnetic scattering by arbitrarily shaped magnetodielectric object," *IEEE Trans. Antennas Propagat.*, Vol. 55, No. 7, 2073–2079, Jul. 2007.
17. Phillips, J. R. and J. White, "A precorrected-FFT method for capacitance extraction of complicated 3-D structures," *Proc. of Int. Conf. on Computer-aided Design*, 268–271, 1994.
18. Phillips, J. R. and J. K. White, "A precorrected-FFT method for electrostatic analysis of complicated 3-D structures," *IEEE Transactions on Computer-aided Design of Integrated Circuits and Systems*, Vol. 16, No. 10, 1059–1072, Oct. 1997.
19. Nie, X., L. W. Li, N. Yuan, and T. S. Yeo, "Fast analysis of scattering by arbitrarily shaped three-dimensional objects using the precorrected-FFT method," *Microwave Opt. Technol. Lett.*, Vol. 34, No. 6, 438–442, Sep. 2002.
20. Nie, X.-C., L.-W. Li, and N. Yuan, "Precorrected-FFT algorithm for solving combined field integral equations in electromagnetic scattering," *Journal of Electromagnetic Waves and Applications*, Vol. 16, No. 8, 1171–1187, 2002.
21. Nie, X. C., L. W. Li, N. Yuan, T. S. Yeo, and Y. B. Gan, "A fast analysis of electromagnetic scattering by arbitrarily shaped homogeneous dielectric objects," *Microwave Opt. Technol. Lett.*, Vol. 38, No. 1, 30–35, Jul. 2003.
22. Nie, X.-C., N. Yuan, L.-W. Li, T.-S. Yeo, and Y.-B. Gan, "Fast analysis of electromagnetic transmission through arbitrarily shaped airborne radomes using precorrected-FFT method," *Progress In Electromagnetics Research*, PIER 54, 37–59, 2005.
23. Yuan, N., T. S. Yeo, X. C. Nie, L. W. Li, and Y. B. Gan, "Analysis of scattering from composite conducting and dielectric targets using the precorrected-FFT algorithm," *Journal of Electromagnetic Waves and Applications*, Vol. 17, No. 3, 499–515, 2003.
24. Nie, X.-C., N. Yuan, L.-W. Li, Y.-B. Gan, and T.-S. Yeo, "A fast volume-surface integral equation solver for scattering from composite conducting-dielectric objects," *IEEE Trans. Antennas Propagat.*, Vol. 53, No. 2, 818–824, Feb. 2005.
25. Nie, X.-C., L.-W. Li, N. Yuan, T.-S. Yeo, and Y.-B. Gan, "Precorrected-FFT solution of the volume integral equation for 3-D inhomogeneous dielectric objects," *IEEE Trans. Antennas Propagat.*, Vol. 53, No. 1, 313–320, Jan. 2005.
26. Nie, X.-C., N. Yuan, L.-W. Li, Y.-B. Gan, and T.-S. Yeo, "A fast combined field volume integral equation solution to EM

scattering by 3-D dielectric objects of arbitrary permittivity and permeability," *IEEE Trans. Antennas Propagat.*, Vol. 54, No. 3, 961–969, Mar. 2006.

27. Zhang, L., N. Yuan, M. Zhang, L.-W. Li, and Y.-B. Gan, "RCS computation for a large array of waveguide slots with finite wall thickness using the mom accelerated by P-FFT algorithm," *IEEE Trans. Antennas Propagat.*, Vol. 53, No. 9, 3101–310, Sep. 2005.
28. Zhang, M., L.-W. Li, and A.-Y. Ma, "Analysis of scattering by a large array of waveguide-fed wide-slot millimeter wave antennas using precorrected-FFT algorithm," *IEEE Microwave and Wireless Components Letters*, Vol. 15, No. 11, 772–774, Nov. 2005.
29. Nie, X. C., Y. B. Gan, N. Yuan, C.-F. Wang, and L.-W. Li, "An efficient hybrid method for analysis of slot array enclosed by a large radome," *Journal of Electromagnetic Waves and Applications*, Vol. 20, No. 2, 249–264, Feb. 2006.
30. Yuan, N., X. C. Nie, Y. B. Gan, T.-S. Yeo, and L.-W. Li, "Accurate analysis of conformal antenna arrays with finite and curved frequency selective surfaces," *Journal of Electromagnetic Waves and Applications*, Vol. 21, No. 13, 1745–1760, Dec. 2007.
31. Suter, E. and J. Mosig, "A subdomain multilevel approach for the MoM analysis of large planar antennas," *Microwave Opt. Technol. Lett.*, Vol. 26, 270–277, Aug. 2000.
32. Matekovits, L., V. Laza, and G. Vecchi, "Analysis of large complex structures with the synthetic-functions approach," *IEEE Trans. Antennas Propagat.*, Vol. 55, No. 9, 2509–2521, Sep. 2007.
33. Prakash, V. V. S. and R. Mittra, "Characteristic basis function method: A new technique for efficient solution of method of moments matrix equations," *Microwave Opt. Technol. Lett.*, Vol. 36, 95–100, Jan. 2003.
34. Yeo, J., V. V. S. Prakash, and R. Mittra, "Efficient analysis of a class of microstrip antennas using the characteristic basis function method (CBFM)," *Microwave Opt. Technol. Lett.*, Vol. 39, 456–464, 2003.
35. Maaskant, R., R. Mittra, and A. Tijhuis, "Fast analysis of large antenna arrays using the characteristic basis function method and the adaptive cross approximation algorithm," *IEEE Trans. Antennas Propagat.*, Vol. 56, 3440–3451, Nov. 2008.
36. Lu, W., T. Cui, Z. Qian, X. Yin, and W. Hong, "Accurate analysis of large-scale periodic structures using an efficient sub-entiredomain basis function method," *IEEE Trans. Antennas Propagat.*, Vol. 52, No. 11, 3078–3085, Nov. 2004.

37. Lu, W. B., T. J. Cui, X. X. Yin, Z. G. Qian, and W. Hong, "Fast algorithms for large-scale periodic structures using subentire domain basis functions," *IEEE Trans. Antennas Propagat.*, Vol. 53, No. 3, 1154–1162, Mar. 2005.
38. Lu, W. B., T. J. Cui, and H. Zhao, "Acceleration of fast multipole method for large-scale periodic structures with finite sizes using sub-entire-domain basis functions," *IEEE Trans. Antennas Propagat.*, Vol. 55, No. 2, 414–421, Feb. 2007.